

Interfractional Displacement Analysis of the Spinal Cord for 21 Head & Neck Cases in Radiation Therapy Planning

Armin Stoll¹, Kristina Giske¹, Eva Stoiber², Rolf Bendl^{1,3}

¹Medical Physics in Radiation Oncology, DKFZ Heidelberg

²Clinical Cooperation Unit Radiation Oncology, DKFZ Heidelberg

³Medical Informatics, Heilbronn University

a.stoll@dkfz-heidelberg.de

Abstract. A monomodal slice-based displacement analysis of the spinal cord for three-dimensional computer tomography imaging in radiation therapy planning is presented. In total, 21 head and neck cases with tumor indications close to the spinal cord are studied and evaluated. Two-dimensional cross-correlation is applied to propagate manually segmented contours of the spinal cord from a high-resolution planning CT to subsequently acquired control CTs. The method and the fully automatic implementation turned out to be reliable and robust. A very few manual corrections on the resulting contours remained necessary in single transversal slices.

1 Introduction

A main effort to fractional radiation therapy is to achieve high tumor control probability with minimal risk of side effects during several weeks of cancer treatment with ionizing radiation [1]. Adaptive radiation therapy is therefore in the focus of research to conform precise radiation dose distributions to a cancerous target volume [2, 3]. To overcome inter- and intrafractional motion uncertainties, margins of the gross tumor volume are increased and adapted according to physicians' expertise. A monomodal displacement analysis of the spinal cord in computer tomography imaging along the longitudinal axis is presented in this contribution. As a result, a multiplicity of non-rigid interfractional organ motions are seen, even though individually adjusted immobilization techniques are applied. The displacement of the spinal cord is automatically determined by propagating manually segmented contours of the spinal cord from the treatment planning computer tomogram (TPCT) to several control computer tomograms (CCTs) by applying two-dimensional cross-correlation per transversal slice [4].

2 Material and methods

Twenty-one head and neck cases are studied in this retrospective investigation and the displacement of the spinal cord in lateral (L) and anterior-posterior

(AP) direction during several weeks of radiation therapy treatment is evaluated. Variances along L and AP directions are additionally derived.

Each case comprises one TPCT and several CCTs (4-11; mean $\mu = 6.6$). All TPCTs (acquired by a Toshiba Aquilion[®] CT scanner) and CCTs (mainly acquired by a Siemens Somatom Emotion[®] CT scanner – within the treatment room) have spatial resolutions of 512×512 voxels (voxel size: $1 \times 1 \times 3$ mm). A TPCT covers the whole volume of interest from the human anatomy (> 100 slices) while all CCTs only focus on a specific volume of interest (~ 50 slices) – primarily on the target volume (see Fig. 1). The maximum value of the normalized cross-correlation coefficient $\Theta_{CC} \in [-1, 1]$ is evaluated as a measure for similarity between a template patch A from the TPCT and a search region B within the CCTs after transformation T :

$$\Theta_C = \sum_{\mathbf{x} \in \Omega_{A,B}^T} (A(\mathbf{x}) - \bar{A})(B^T(\mathbf{x}) - \bar{B}) \quad (1)$$

Apart from the subtraction of the image mean values \bar{A} and \bar{B} , the cross-correlation coefficient Θ_C in equation (1) describes a convolution of two images. A convolution can be calculated in an efficient way in its Fourier domain. Both image-patches (the zero-padded template from the TPCT and the search region from a given CCT) are therefore transformed into the Fourier domain. The calculation then turns into a multiplication of both images. The inverse Fourier transformation leads to all correlation coefficients and enables an fast estimation of the displacement of the spinal cord within the CCT:

$$\Theta_C = \mathbf{FFT}^{-1}(\mathbf{FFT}(\Omega_A) \cdot \mathbf{FFT}(\Omega_B)^*) \quad (2)$$

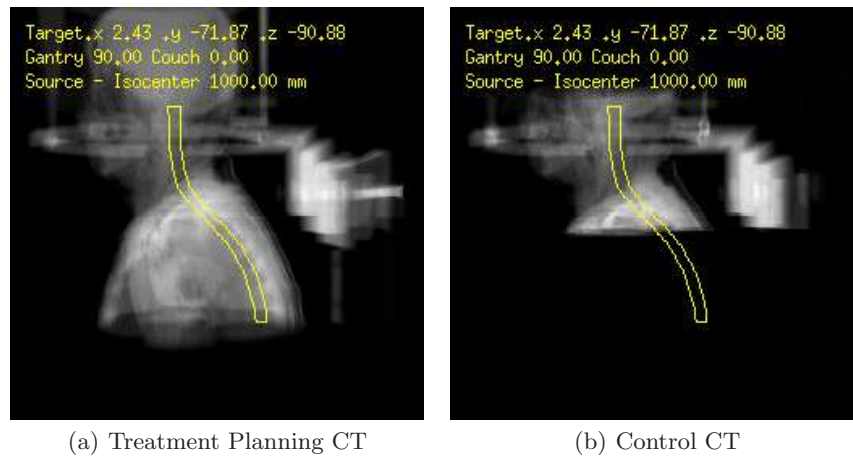


Fig. 1. Visualization: digitally reconstructed radiographs (DRR) in lateral direction

Finally, the correlation coefficients Θ_C are divided by the square root of the auto-correlation product of both images, to obtain normalized correlation coefficients:

$$\Theta_{CC} = \frac{\Theta_C(A, B^T)}{\sqrt{\Theta_C(A, A) \cdot \Theta_C(B^T, B^T)}} \quad (3)$$

All rectangular templates, with image contents according to the manually segmented contours of the spinal cord in the TPCT, are derived from minimum and maximum vertices along L and AP direction. The template size is constantly increased in both direction by 20 voxels ($\sim 20\text{mm}$), with intention to enhance robustness of the cross-correlation calculation (see Fig. 2(a)).

Since all CCTs per case are stereotactically registered according to the TPCT, a global coordinate system is given for every CCT and therefore the relative template position in the TPCT serves as initial search region within the CCTs, too. The initial search region in each CCT is additionally enlarged by 15 voxels ($\sim 15\text{mm}$) in L and AP direction (see Fig. 2(b)). This area seemed to be suitable to cover large displacements without overestimating the search volume. The maximum cross-correlation coefficient finally indicates similar image content in the TPCT and CCT and therefore implicitly enables to estimate the displacement of the spinal cord within a slice (see Fig. 2(c)).

3 Results

Using this approach, 7573 contours of the spinal cord from 21 head and neck cases were adapted to 138 CCTs in every single transversal slice (see Table 1). Seventeen false propagation results within single transversal slices were immediately identified during the calculations and instantly reported for subsequent manual corrections. As error criterion, a displacement $> 13\text{ mm}$ in one directions was assumed. After three-dimensional visualization of all resulting contours, 14

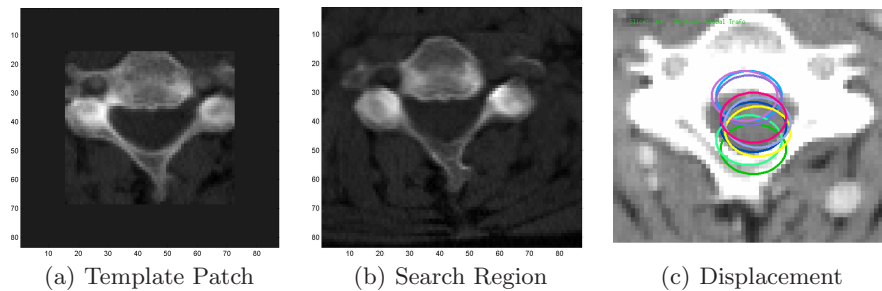


Fig. 2. Examples: Fig. 2(a) shows a zero-padded template patch. It is identified in every transversal slice of the TPCT around the spinal cord. Fig. 2(b) demonstrates that a similar pattern is expected to occur in the CCTs within an extended search region. Fig. 2(c) gives an example of the displacement of the spinal cord within one slice.

Table 1. Detailed evaluation of all 21 head and neck cases without error correction

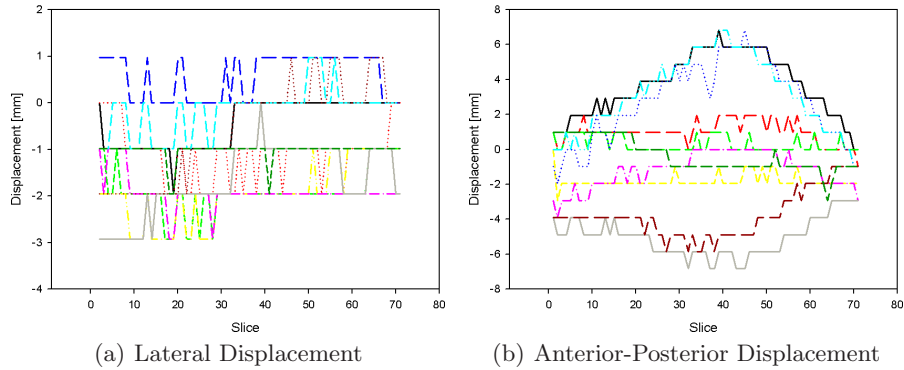
Case	#CCTs	Err. Det.	Man. Cor.	\bar{x} [mm]	\bar{y} [mm]	σ_x^2 [mm]	σ_y^2 [mm]	#Contours
1	5	0	0	-0,12	-0,61	0,22	0,87	292
2	7	0	0	0,39	2,67	0,95	10,32	388
3	8	0	0	-3,12	0,12	4,07	2,24	432
4	9	0	1	-2,20	-2,06	2,93	10,8	451
5	4	1	3	-0,55	-0,01	1,66	2,73	262
6	7	0	0	-0,36	-0,42	0,83	1,97	426
7	8	2	2	3,70	-0,22	5,44	1,67	446
8	4	0	0	-0,96	-0,85	1,16	0,62	182
9	7	0	0	-1,84	-0,83	1,46	1,40	411
10	6	0	0	-1,43	2,15	0,99	1,94	301
11	6	0	3	0,71	-1,79	1,02	5,64	343
12	8	0	2	-0,34	-0,99	1,55	1,28	440
13	5	0	0	0,71	-0,17	4,87	0,95	255
14	11	0	0	-1,72	0,37	1,84	1,04	599
15	7	0	0	0,08	-0,47	0,81	2,21	327
16	5	0	3	-0,07	-0,62	0,15	0,98	265
17	5	0	0	-1,23	-1,13	6,57	5,80	323
18	9	12	14	0,72	0,02	5,65	10,65	459
19	6	2	3	0,05	-0,20	2,21	3,56	296
20	5	0	0	2,20	-0,56	2,41	1,90	314
21	6	0	0	-0,89	-0,27	1,71	2,37	361
Sum	138	17	31					7573

additional false propagation results were identified in a few slices and necessary to manually correct. In summary, 31 outliers are corrected manually after the fully automatic propagation. These outliers occurred due to image artifacts, CCT range limitations or crucial superior-interior displacements of a vertebral body.

4 Conclusion

A multiplicity of non-rigid L and AP displacements along the spinal cord are observed (see Fig. 3). For this reason, patient positioning after rigid image registration can remain insufficient for head and neck cases in radiation therapy treatment. Single non-rigid displacements could eventually cause serious adverse effects when the spinal cord extends high radiation dose volumes. In particular, when target volumes and spinal cord are located in close proximity to each other. It is therefore considered to apply elastic image registration algorithms in this body region [5, 6, 7] instead of rigid ones. Elastic image registration

Fig. 3. One head and neck case with severe non-rigid displacements of the spinal cord in AP direction – along the longitudinal axis.



eventually can reveal non-rigid displacements of the spinal cord and help to correct them. An other strategy could be to apply spine segmentation [8] to detect displacements at an early stage and correct them if necessary, too.

References

1. Schlegel W, Mahr A. 3D conformal radiation therapy. Berlin Heidelberg New York: Springer Verlag; 2001. A multimedia introduction to methods and techniques.
2. Hysing LB, Skorpen TN, Alber M, et al. Influence of organ motion on conformal vs. intensity-modulated pelvic radiotherapy for prostate cancer. *Int J Radiat Oncol Biol Phys.* 2009;71(5):1496–503.
3. Moser T, Biederer J, Nill S, et al. Detection of respiratory motion in fluoroscopic images for adaptive radiotherapy. *Phys Med Biol.* 2008;53(12):3129–45.
4. Maintz JB, Viergever MA. A survey of medical image registration. *Med Image Anal.* 1998;2(1):1–36.
5. Li P, Malsch U, Bendl R. Combination of intensity-based image registration with 3D simulation in radiation therapy. *Phys Med Biol.* 2008;53(17):4621–4637.
6. Malsch U, Thieke C, Bendl R. Fast elastic registration for adaptive radiotherapy. *Comput Assist Interv.* 2006;9(2):612–9.
7. Floca RO, Metzner R, Wirtz CR, et al. Entwicklung und Optimierung eines elastischen Registrierungsverfahrens für CTA und RA Daten. *Procs BVM.* 2008; p. 133–137.
8. Klinder T, Wolz R, Lorenz C, et al. Spine segmentation using articulated shape models. *Proc MICCAI.* 2008; p. 227–234.